This article was downloaded by: [Renmin University of China]
On: 13 October 2013, At: 10:49
Publisher: Taylor & Francis
Informa Ltd Registered in England and Wales Registered Number: 1072954 Registered office: Mortimer House, 37-41 Mortimer Street, London W1T 3JH, UK

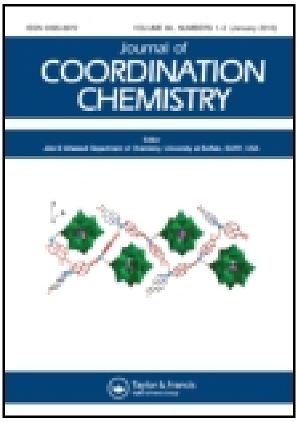

Journal of Coordination Chemistry
Publication details, including instructions for authors and subscription information:
http://www.tandfonline.com/loi/gcoo20

Copper(II) coordination polymers constructed from aromatic polycarboxylate and flexible triazole ligands with different spacer lengths: syntheses, structures, and properties

Li Tian [a] & Shang Yong Zhou [a]

[a] Tianjin Key Laboratory of Structure and Performance for Functional Molecules, Key Laboratory of Inorganic-Organic Hybrid Functional Material Chemistry, Ministry of Education , College of Chemistry, Tianjin Normal University , Tianjin , China

Accepted author version posted online: 21 Jun 2013.Published online: 22 Jul 2013.

To cite this article: Li Tian & Shang Yong Zhou (2013) Copper(II) coordination polymers constructed from aromatic polycarboxylate and flexible triazole ligands with different spacer lengths: syntheses, structures, and properties, Journal of Coordination Chemistry, 66:16, 2863-2874, DOI: 10.1080/00958972.2013.818138

To link to this article: http://dx.doi.org/10.1080/00958972.2013.818138

PLEASE SCROLL DOWN FOR ARTICLE

Taylor & Francis makes every effort to ensure the accuracy of all the information (the "Content") contained in the publications on our platform. However, Taylor & Francis, our agents, and our licensors make no representations or warranties whatsoever as to the accuracy, completeness, or suitability for any purpose of the Content. Any opinions and views expressed in this publication are the opinions and views of the authors, and are not the views of or endorsed by Taylor & Francis. The accuracy of the Content should not be relied upon and should be independently verified with primary sources of information. Taylor and Francis shall not be liable for any losses, actions, claims, proceedings, demands, costs, expenses, damages, and other liabilities whatsoever or howsoever caused arising directly or indirectly in connection with, in relation to or arising out of the use of the Content.

This article may be used for research, teaching, and private study purposes. Any substantial or systematic reproduction, redistribution, reselling, loan, sub-licensing, systematic supply, or distribution in any form to anyone is expressly forbidden. Terms &

Journal of Coordination Chemistry, 2013
Vol. 66, No. 16, 2863–2874, http://dx.doi.org/10.1080/00958972.2013.818138

Copper(II) coordination polymers constructed from aromatic polycarboxylate and flexible triazole ligands with different spacer lengths: syntheses, structures, and properties

LI TIAN* and SHANG YONG ZHOU

Tianjin Key Laboratory of Structure and Performance for Functional Molecules, Key Laboratory of Inorganic–Organic Hybrid Functional Material Chemistry, Ministry of Education, College of Chemistry, Tianjin Normal University, Tianjin, China

(*Received 17 January 2013; in final form 18 May 2013*)

$\{[Cu_2(btm)_2(Hbtc)(H_2btc)_2(H_2O)]\cdot 9.5H_2O\}_n$ (**1**), $[Cu(bte)(H_2btc)_2]_n$ (**2**) $\{[Cu(btp)(H_2btc)_2]\cdot 0.25H_2O\}_n$ (**3**) (btm = bis(1,2,4-triazol-1-yl)methane, bte = bis(1,2,4-triazol-1-yl)ethane, btp = bis(1,2,4-triazol-1-yl)propane, H_3btc = benzene-1, 3, 5-tricarboxylic acid) have been synthesized and structurally characterized. **1** features a 1-D double chain, which is interconnected by classical hydrogen-bonding (O–H···O) and π–π interactions to lead to a 3-D supramolecular architecture. **2** and **3** are both 1-D single chains, which are interconnected by π–π interactions to 2-D layer architectures. Elemental analysis, XRD, IR, TG and EPR spectra have been carried out and discussed.

Keywords: H_3btc; Bis(1,2,4-triazol-1-yl)methane; Bis(1,2,4-triazol-1-yl)ethane; Bis(1,2,4-triazol-1-yl)propane; EPR spectra

1. Introduction

Metal coordination polymers have interesting topologies and potential applications in areas such as catalysis, adsorption (gas storage), luminescence, and magnetism [1–9]. A key step for construction of polymeric transition metal complexes is to select appropriate multidentate bridging ligands [10, 11]. Flexible bispolyazole-type ligands such as 1- or 4-substituted 1,2,4-triazole rings tethered by an alkyl spacer can be used to obtain a variety of polynuclear molecules and linear coordination polymers [12–15]. The flexibility and conformational freedom of bispolyazole ligands can offer the possibility for construction of unpredictable and interesting frameworks.

Owing to the diversity of coordination modes and high structural stabilities, multicarboxylic ligands with suitable spacers, especially benzoic acid – based ligands, are frequently used for metal-organic networks [16–21]. Benzene-1,3,5-tricarboxylic acid (H_3btc, also known as trimesic acid) is a rigid, planar molecule that has been widely used as a bridging ligand in the synthesis of multidimensional MOFs.

---

*Corresponding author. Emails: hxxytl@mail.tjnu.edu.cn, lilytianli@hotmail.com

We reported crystal structures of a series of transition metal coordination polymers (Cd^{2+}, Zn^{2+}, Cu^{2+}, and Co^{2+}) with flexible bis(triazole) ligands [22–25]. In this contribution, we choose bis(1,2,4-triazol-1-yl)methane (btm), bis(1,2,4-triazol-1-yl)ethane (bte), and bis(1,2,4-triazol-1-yl)propane (btp) with benzene-1,3,5-tricarboxylic acid as building blocks. Three coordination polymers, $\{[Cu_2(btm)_2(Hbtc)(H_2btc)_2(H_2O)]\cdot 9.5H_2O\}_n$ (**1**), $[Cu(bte)(H_2btc)_2]_n$ (**2**) and $\{[Cu(btp)(H_2btc)_2]\cdot 0.25H_2O\}_n$ and (**3**), were fabricated and structurally characterized by X-ray single-crystal analyses. IR spectra, thermal stabilities, and EPR spectra are also discussed.

2. Experimental

2.1. *General remarks*

Deionized water was used as solvent in this study. The reagents and solvents employed were commercially available and used as received without purification. Ligands btm, bte, and btp were synthesized as reported previously [26]. Elemental analyses (C, H, and N) were carried out on a Perkin–Elmer elemental analyzer. FT-IR spectra were recorded from KBr pellets (4000–400 cm^{-1}) on a Bio-Rad FTS 135 spectrometer. Powder X-ray diffraction measurements were recorded on a D/Max-2500 X-ray diffractometer using Cu-Kα radiation. TG experiments were performed on a NETZSCH TG 209 instrument with a heating rate of 10 °C min^{-1} under nitrogen. EPR spectra were measured on a BRUKER EMX-6/1 EPR spectrometer.

Table 1. Crystallographic data and structure refinement details for **1–3**.

Complex	**1**	**2**	**3**
Formula	$C_{37}H_{47}Cu_2N_{12}O_{28.5}$	C_{24} $H_{18}CuN_6O_{12}$	$C_{25}H_{20.5}CuN_6O_{12.25}$
Mr	1242.95	645.99	664.52
Crystal system	$P2_1/n$	P-1	$C2/c$
Space group	Monoclinic	Triclinic	Monoclinic
Temperature (K)	293(2)	293(2)	293(2)
a (Å)	19.8793(13)	7.1318(10)	6.6211(9)
b (Å)	12.0106(5)	9.1002(14)	24.283(3)
c (Å)	22.6318(13)	10.5135(16)	16.819(2)
α (°)	90	77.539(13)	90
β (°)	112.323(7)	70.630(13)	97.681(14)
γ (°)	90	89.441(12)	90
V (Å^3)	4998.7(5)	627.13(16)	2679.9(6)
Z, ρcalc (Mg/m^3)	4, 1.652	1, 1.710	4, 1.647
M (mm^{-1})	0.958	0.953	0.895
F (000)	2556	329	1358
θ range (°)	2.42–25.01	2.75–25.00	2.44–25.01
Limiting indices	$-18 \leqslant h \leqslant 23$ $-14 \leqslant k \leqslant 14$ $-26 \leqslant l \leqslant 26$	$-5 \leqslant h \leqslant 8$ $-10 \leqslant k \leqslant 10$ $-7 \leqslant l \leqslant 12$	$-7 \leqslant h \leqslant 7$ $-19 \leqslant k \leqslant 28$ $-19 \leqslant l \leqslant 19$
Reflections collected/unique	28,515/8783	1867/1516	5039/2367
R (int)	0.0260	0.0185	0.0243
Goodness-of-fit on F^2	1.135	1.062	1.088
R_1/wR_2 [$I > 2\sigma(I)$]	$R_1 = 0.0452$, $wR_2 = 0.1369$	$R_1 = 0.0328$, $wR_2 = 0.0871$	$R_1 = 0.0330$, $wR_2 = 0.0900$
R_1/wR_2 (all data)	$R_1 = 0.0619$ $wR_2 = 0.1440$	$R_1 = 0.0343$, $wR_2 = 0.0880$	$R_1 = 0.0402$, $wR_2 = 0.0928$
Largest diff. peak and hole (e Å^{-3})	1.422 and −0.932	0.324 and −0.322	0.497 and −0.521

2.2. *Synthesis of* $\{[Cu_2(btm)_2(Hbtc)(H_2btc)_2(H_2O)]\cdot 9.5H_2O\}_n$ *(1),* $[Cu(bte)(H_2btc)_2]_n$ *(2), and* $\{[Cu(btp)(H_2btc)_2]\cdot 0.25H_2O\}_n$ *(3)*

Complexes **1**, **2,** and **3** were prepared by the following method: a mixture of $Cu(NO_3)_2$ (154.24 mg, 0.5 mM), benzene-1,3,5-tricarboxylic acid (106.5 mg, 0.5 mM), bis-triazole (0.5 mM, btm for **1**; bte for **2** and btp for **3**), NEt_3 (1.0 mM), and H_2O (12 mL) into a Parr Teflon-lined stainless steel vessel (25 mL), then the vessel was sealed, heated to 140 °C and kept for 3 days. The autoclave was cooled to room temperature at $1.5\,°C\,h^{-1}$. Blue crystalline products **1–3** were filtered off, washed with distilled water, and dried in air.

For **1**: Yield: 38% (based on Cu). Anal. Calcd for $C_{37}H_{47}Cu_2N_{12}O_{28.5}$ (**1**) (%): C, 35.75; H, 3.78; N, 13.52. Found: C, 35.84; H, 3.35; N, 13.02.

For **2**: Yield: 32% (based on Cu). Anal. Calcd for $C_{24}\ H_{18}CuN_6O_{12}$ (**2**) (%): C, 39.48; H, 2.49; N, 23.03. Found: C, 39.69; H, 2.79; N, 23.52.

For **3**: Yeld: 35% (based on Cu). Anal. Calcd for $C_{25}H_{20.5}CuN_6O_{12.25}$ (**3**) (%): C, 45.18; H, 3.11; N, 12.65. Found: C, 45.62; H, 3.27; N, 12.22.

2.3. *X-ray crystallography*

Single-crystal X-ray diffraction measurements of **1–3** were carried out with a Bruker Smart CCD diffractometer and a graphite crystal monochromator situated in the incident beam for data collection at room temperature. Lorentz polarization and absorption corrections

Table 2. Selected bond lengths (Å) and angles (°) for **1–3**.

1			
Cu(1)–O(1)	1.955(2)	O(1)–Cu(1)–N(7)	91.31(9)
Cu(1)–O(7)	1.990(2)	O(7)–Cu(1)–N(7)	89.49(10)
Cu(1)–N(7)	1.995(3)	O(1)–Cu(1)–N(1)	90.50(9)
Cu(1)–N(1)	2.009(3)	O(7)–Cu(1)–N(1)	88.80(10)
Cu(1)–O(19)	2.345(2)	N(7)–Cu(1)–N(1)	177.82(10)
Cu(2)–O(3)#1	1.970(2)	O(1)–Cu(1)–O(19)	93.63(8)
Cu(2)–N(6)#2	1.979(3)	O(7)–Cu(1)–O(19)	90.81(9)
Cu(2)–N(12)	1.992(3)	N(12)–Cu(2)–O(13)	89.08(10)
Cu(2)–O(13)	1.997(2)	O(3)#1–Cu(2)–N(12)	90.49(9)
O(1)–Cu(1)–O(7)	175.49(9)	N(6)#2–Cu(2)–N(12)	176.90(11)
2			
Cu(1)–N(1)#1	1.960(2)	N(1)#1–Cu(1)–O(2)	88.56(8)
Cu(1)–N(1)	1.960(2)	N(1)–Cu(1)–O(2)	91.44(8)
Cu(1)–O(1)#1	1.986(2)	O(1)#1–Cu(1)–O(2)	124.30(7)
Cu(1)–O(1)	1.986(2)	O(1)–Cu(1)–O(2)	55.70(7)
Cu(1)–O(2)	2.604(2)	N(1)#1–Cu(1)–O(2)#1	91.44(8)
Cu(1)–O(2)#1	2.604(2)	N(1)–Cu(1)–O(2)#1	88.56(8)
N(1)#1–Cu(1)–N(1)	180.00(14)	N(1)–Cu(1)–O(1)#1	91.38(9)
N(1)#1–Cu(1)–O(1)#1	88.62(9)		
3			
Cu(1)–O(1)#1	1.9670(15)	O(1)#1–Cu(1)–O(1)	180.00(7)
Cu(1)–O(1)	1.9670(15)	O(1)#1–Cu(1)–N(1)#1	90.79(7)
Cu(1)–N(1)#1	1.9749(19)	O(1)–Cu(1)–N(1)#1	89.21(7)
Cu(1)–N(1)	1.9749(19)	O(1)–Cu(1)–N(1)	90.79(7)

Note: Symmetry transformations used to generate equivalent atoms: **1**, #1 $-x+1$, $-y$, $-z+1$; #2 $x-1$, y, z; **2**, #1 $-x+1$, $-y$, $-z+1$; **3**, #1 $-x+3/2$, $-y+1/2$, $-z$.

were applied. The structures were solved by direct methods and refined by full-matrix least-squares using SHELXS-97 and SHELXL-97. All nonhydrogen atoms were refined anisotropically and hydrogens were located and refined isotropically. Crystallographic data for **1–3** are summarized in table 1. Selected bond distances and angles of **1–3** are listed in table 2.

3. Results and discussion

3.1. *Crystal structure of* $\{[Cu_2(btm)_2(H_2btc)_2(Hbtc)(H_2O)_2]\cdot 9.5H_2O\}_n$ *(1)*

Single-crystal X-ray analysis shows that **1** crystallizes in the monoclinic space group $P2_1/n$ with an asymmetric unit of two Cu(II), two H_2btc^- and one $Hbtc^{2-}$, two btm ligands, and two coordinated waters. As viewed in figure 1, both Cu1 and Cu2 are five-coordinate in a distorted trigonal bipyramidal coordination sphere defined by two nitrogen donors from btm occupying the axial positions, while the equatorial positions are completed by two carboxylic oxygens and one water oxygen. All Cu–O and Cu–N bond lengths fall in the normal range.

In the structure of **1**, Cu(II) ions are bridged by btm (*T*) to construct a wave line with a Cu···Cu distance of 10.196 Å; two such wave lines are interconnected through $Hbtc^{2-}$ to yield a 1-D ladder (figure 2) that is based on the building unit $[Cu_4(btm)_2(Hbtc)_2(H_2btc)_4]$.

The 1-D ladders are further linked via π–π interactions between H_2btc^- and H_2btc^-, or $Hbtc^{2-}$ and H_2btc^-, thus forming a 2-D supramolecular framework, as shown in figure 3.

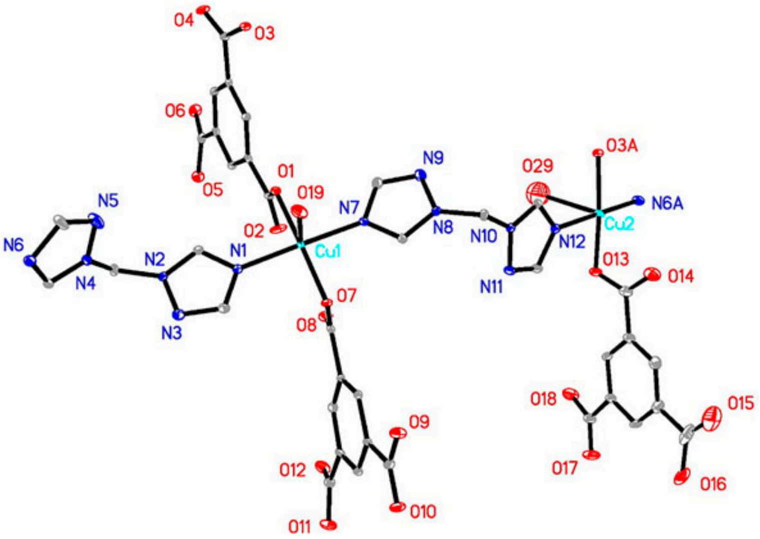

Figure 1. Molecular structure of **1** showing the coordination environments of Cu^{2+}, H_3btc and btm.

3.2. *Crystal structure of [Cu(bte)(H_2btc)$_2$]$_n$ (2)*

When bte was used instead of btm, a new 1-D chain **2** is obtained. **2** crystallizes in the monoclinic space group *C*2/*c* with an asymmetric unit containing half of a Cu(II), one H_2btc^- and half of a bte (figure 4). Unlike **1**, Cu1 is six-coordinate in a distorted octahedral coordination sphere that is defined by two nitrogens from two bte occupying the axial positions, while the equatorial positions are completed by four oxygens from two H_2btc^-. The Cu1–O2 bond distance (2.598(2) Å) is slightly longer than normal Cu–O distances, which can be attributed to Jahn–Teller elongation. All other Cu–O and Cu–N bond lengths fall in the normal range.

The bte ligands exhibit *T* conformations with spacers (N1···N1A = 7.905 Å). Acting as bidentate chelating-bridging ligands, a pair of bte chelate Cu1 by triazolyl N1 donors with Cu···Cu separation of 11.613(4) Å, leading to a 1-D "zigzag" chain (figure 5). In the structure of **2**, carboxylates of H_2btc^- have η–O, O′ coordination. On each side of the 1-D chain, H_2btc^- ligands lie exactly parallel. The $\pi\cdots\pi$ interactions between H_2btc^- ligands make **2** a 2-D (4,4) supermolecular layer, as shown in figure 6. The parallel 2-D layers are stacked in an offset fashion to give a 3-D supramolecular architecture with interlayer O3–H3B···O1 and O5–H5A···O6 interactions, as shown in figure 7.

3.3. *Crystal structure of {[Cu(btp)(H_2btc)$_2$]·0.25H_2O}$_n$ (3)*

Complex **3** crystallizes in the triclinic space group *P*-1 with an asymmetric unit containing half of a Cu(II), one H_2hip^- and half of a btp (figure 8). Like **2**, Cu(II) is six-coordinate in a distorted octahedral coordination sphere that is defined by two nitrogens from two btp occupying axial positions, while the equatorial positions are four oxygen donors from two H_2btc^-. The Cu1–O2 bond distance (2.775(2) Å) is longer than the normal Cu–O distances, so the coordination environment of copper can be described as the "4 + 2" coordination mode. The btp is a *GG* conformation with dihedral angles of 86.9° between the two triazole rings.

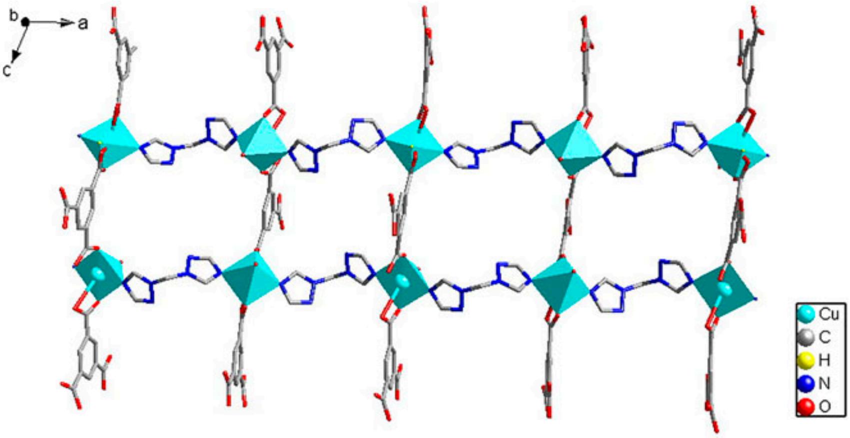

Figure 2. The 1-D ladder structure of **1** linked by H_3btc and btm.

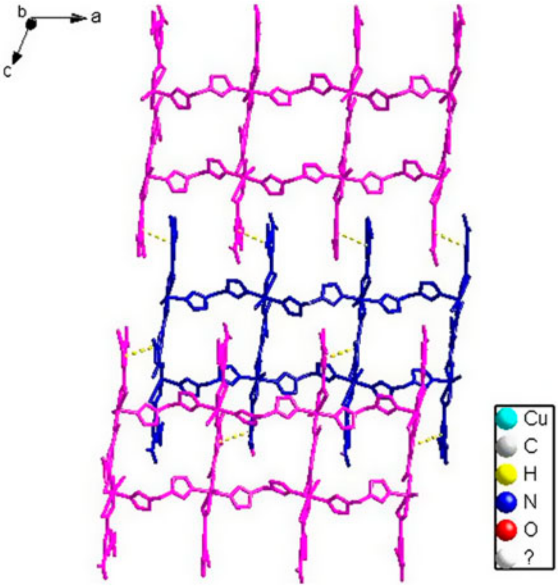

Figure 3. The 2-D supramolecular framework of **1** viewed along the *b* direction via $\pi\cdots\pi$ interactions (yellow dotted line) (see http://dx.doi.org/10.1080/00958972.2013.818138 for color version).

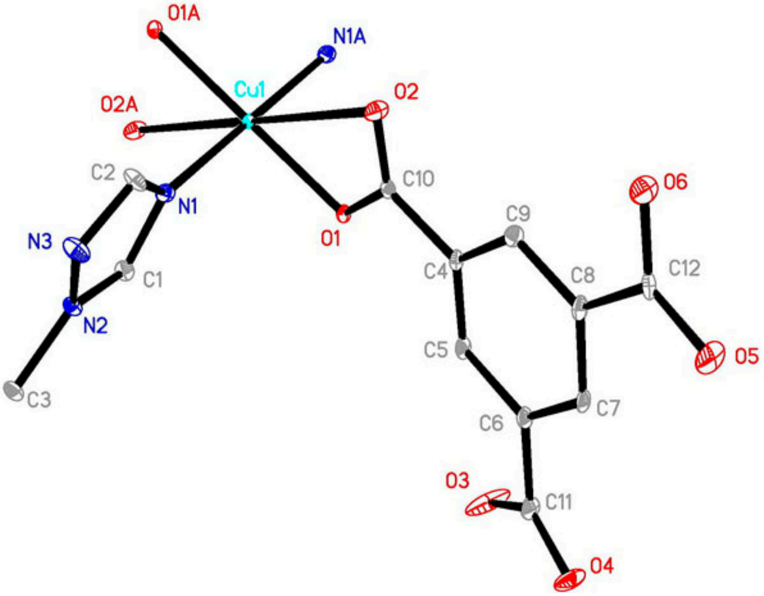

Figure 4. Molecular structure of **2** showing the coordination environments of Cu^{2+}, H_3btc, and bte.

The btp adopt μ_2, linking two Cu(II) ions to construct a 1-D “S-shaped” chain (figure 9). The Cu···Cu separation across the bridging btp ligand is 12.126 Å, ca. 0.5 Å longer than that in **2**. Like in **2**, the carboxylates of H_2btc^- in **2** also have η–O, O′ coordination. However,

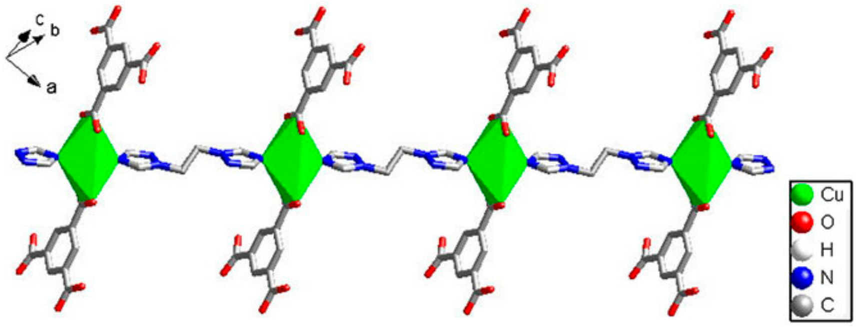

Figure 5. The 1-D chain of **2** linked by bte.

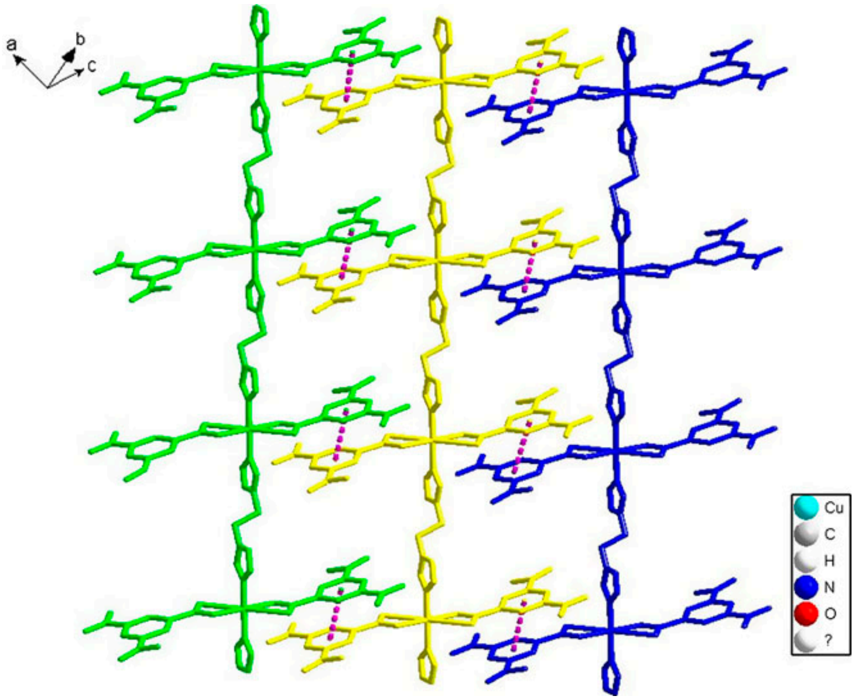

Figure 6. The 2-D supramolecular structure of **2** via $\pi\cdots\pi$ interactions (pink dotted line) (see http://dx.doi.org/10.1080/00958972.2013.818138 for color version).

there are some differences between the 1-D structures of **2** and **3**. On the same side of the 1-D chain, neighboring H_2btc^- ligands lie antiparallel in comparison with that of **2**. The $\pi\cdots\pi$ interactions of the phenyl rings in **3** led to a 2-D step-ladder supramolecular architecture (figure 10). In addition, hydrogen-bonding interactions (table 3) (O3–H3···O2) connect the 2-D layers to give a 3-D supramolecular framework (figure 11).

As illustrated in scheme 1, the architectures for **1–3** mainly result from the bis-triazole ligands with different spacer lengths and conformational flexibility and the deprotonating degree of H_3btc. The btm which employs *T* conformation and $Hbtc^{2-}$ generate a 1-D double-chain structure. The bte employs *T* conformation and H_2btc^- to give **2** as a 1-D

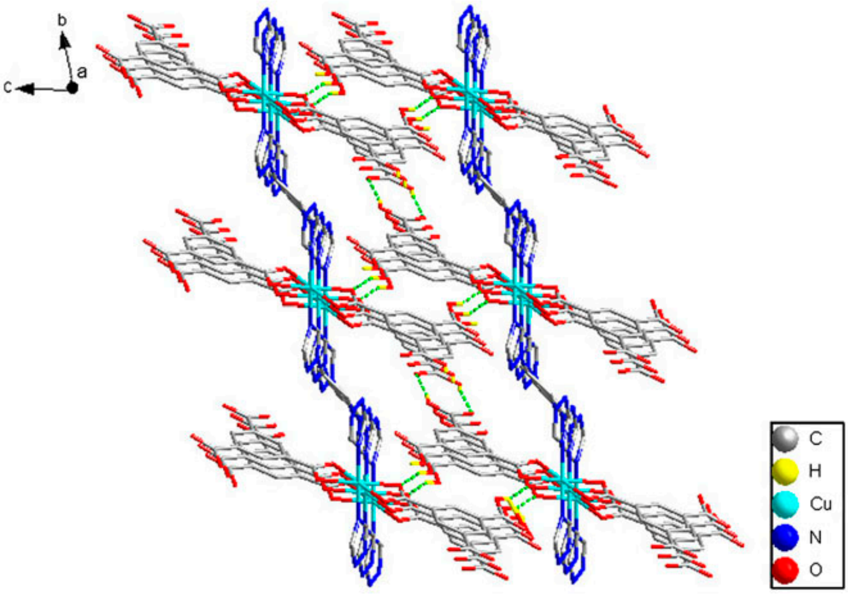

Figure 7. The 3-D supramolecular structure of **2** via O–H· · ·O hydrogen bonds (green dotted line) (see http://dx.doi.org/10.1080/00958972.2013.818138 for color version).

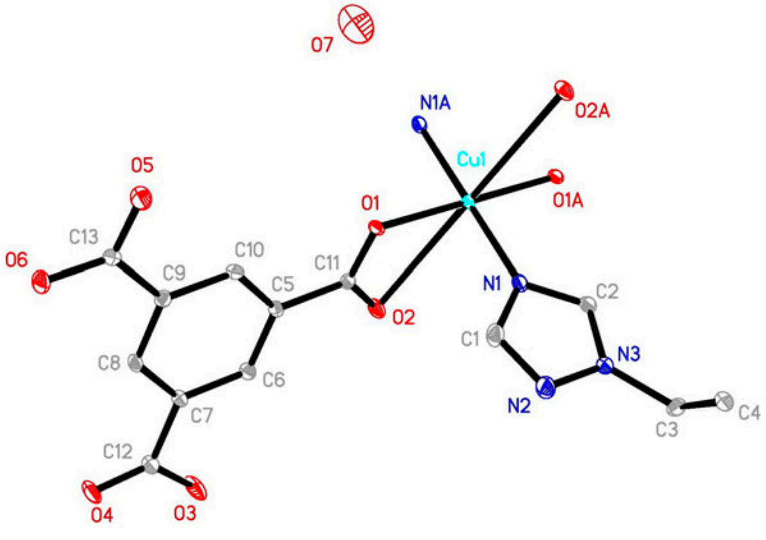

Figure 8. Molecular structure of **3** showing the coordination environments of Cu^{2+}, H_3btc, and btp.

chain. The flexible btp as the *GT* conformation and the H_2btc^- also generates a 1-D chain in **3**. However, **2** and **3** exhibit different patterns and space groups (*P*-1, **2**; *C*2/*c*, **3**) because of the varied conformations of bte and btp. This work can be compared with previous studies [22–25] in which we used flexible bis-triazole and rigid multi-carboxylic ligands and 1-D, 2-D, and 3-D complexes were obtained. In all these complexes, although bis-triazoles adopt the same μ_2 linking mode, ligand conformations, coordination mode of

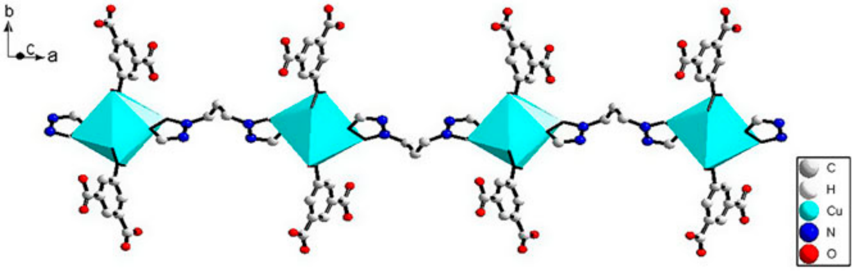

Figure 9. The 1-D chain of **2** linked by btp.

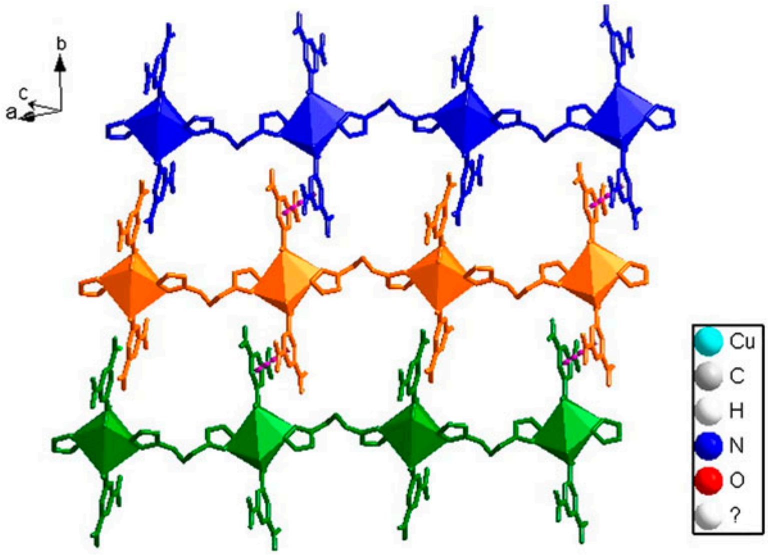

Figure 10. The 2-D supramolecular structure of **3** via $\pi\cdots\pi$ interactions (pink dotted line) (see http://dx.doi.org/10.1080/00958972.2013.818138 for color version).

Table 3. Selected hydrogen bond data for **1–3**.

D–H···A	H···A (Å)	D···A (Å)	D–H···A (°)	Symmetry operation
1				
O5–H5A···O22	1.841	2.647	167.30	
O9–H9A···O20	1.787	2.606	175.91	$-x+3/2,\ y-1/2,\ -z+3/2$
O11–H11···O24	1.767	2.567	164.68	$x+1/2,\ -y+1/2,\ z+1/2$
O16–H16A···O27	1.951	2.684	148.40	$x,\ y-1,\ z+1$
O18–H18···O26	1.782	2.599	174.07	$x,\ y,\ z+1$
O19–H19A···O22	1.918	2.757	172.95	$x,\ y-1,\ z$
O19–H19B···O23	1.953	2.793	170.34	$-x+3/2,\ y-1/2,\ -z+3/2$
2				
O3–H3···O4	1.798	2.617	176.70	$-x-1,\ -y+1,\ -z+2$
O6–H6···O1	1.851	2.625	157.08	$-x+1,\ -y,\ -z+2$
3				
O3–H3···O2	1.797	2.635	164.41	$-x+2,\ -y,\ -z$
O5–H5···O5	1.889	2.612	143.27	$-x,\ y,\ -z+1/2$

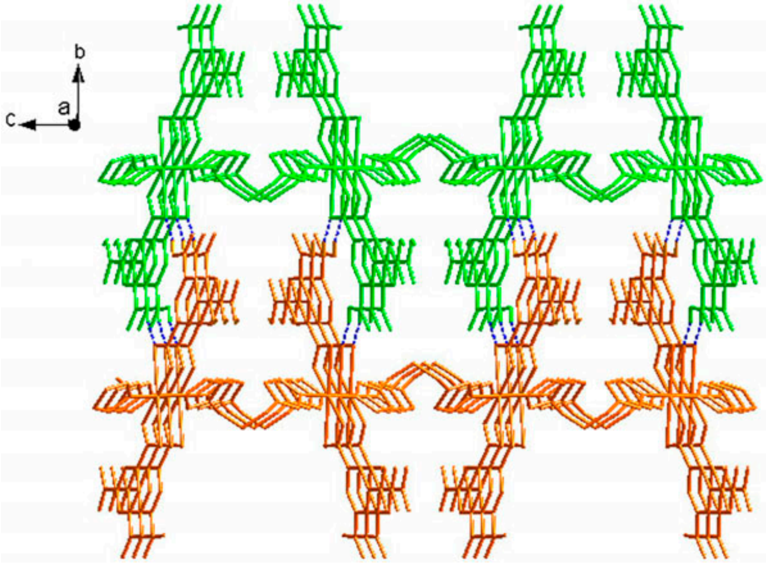

Figure 11. The 3-D supramolecular structure of **3** via O–H· · ·O hydrogen bonds (blue dotted line) (see http://dx.doi.org/10.1080/00958972.2013.818138 for color version).

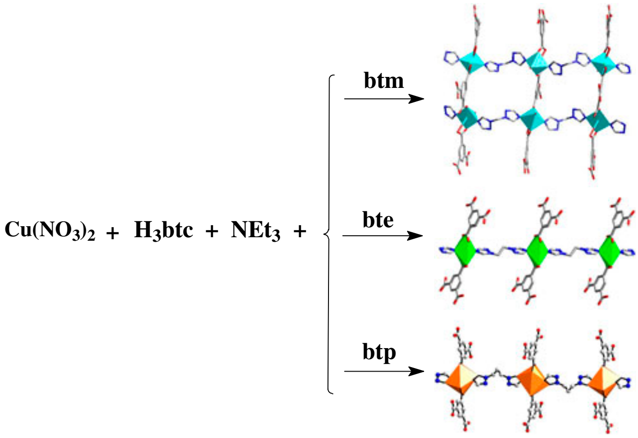

Scheme 1. Synthesis of **1–3**.

the central metal and the deprotonating degree of the aromatic multicarboxylic ligands are important for various framework structures in crystal engineering.

3.4. *IR spectra*

In IR spectra of **1–3** (figures S1–S3), broad peaks centered at ca. 3400 cm^{-1} indicate O–H stretch of water and/or carboxyl. The characteristic absorption band of carboxyl (ca. 1700 cm^{-1}) in **1–3** confirms incomplete deprotonation of aromatic multicarboxylic. As a consequence, the antisymmetric and symmetric stretching vibrations of carboxylate in **1–3** appear at 1570–1530 and 1375–1395 cm^{-1}, respectively.

3.5. *EPR characterization*

EPR spectra of powdered samples of **1**, **2,** and **3** have been measured at room temperature and are shown in figure S4. The simulations were carried out by the EasySpin software [27]. The obtained spectra are characteristic for copper(II) centers, that are simulated assuming axial symmetry of g and A tensors. The simulated spectra were obtained by employing the following parameters: $g_{\|} = 2.18$, $g_{\perp} = 2.07$, $A_{\|} = 50$ and $A_{\perp} = 5\,\mathrm{G}$ for **1**; $g_{\|} = 2.28$, $g_{\perp} = 2.05$, $A_{\|} = 160$ and $A_{\perp} = 10\,\mathrm{MHz}$ for **2** and $g_{\|} = 2.31$, $g_{\perp} = 2.05$ and $A_{\|} = 140$ and $A_{\perp} = 40\,\mathrm{MHz}$ for **3**, respectively. The obtained $g_{\|} > g_{\perp} > 2.0023$ values for both samples point out that the unpaired electron is located in the $d_{x^2-y^2}$ ground state, which is in agreement with the crystal structure and the square-pyramidal coordination around Cu. From the EPR of the two Cu(II) complexes, no half-field signals were observed at RT. So they cannot show strong magnetic interaction.

3.6. *Thermal analyses*

The thermal behaviors of the crystalline materials were studied by thermogravimetric analysis (TGA) under nitrogen, with the thermogravimetric curves shown in figure S6. The TGA results of **1** display two-step weight losses, the first of 15.00% from 50 to 168 °C (Calcd 15.15%) should be attributed to loss of free and coordinated water, and the second is ascribed to loss of the ligands when the temperature is above 260 °C. As for **2** and **3**, very rapid weight losses occur at 230 and 250 °C, respectively, with effectively single-stage weight losses.

4. Conclusion

By using flexible btm, bte, or btp with benzene-1,3,5-tricarboxylic acid (H_3btc), three inoganic–organic frameworks have been constructed under hydrothermal conditions. The diversity of architectures for **1–3** mainly results from the bis-triazole ligands with different spacer lengths and conformational flexibility and the deprotonation degree of H_3btc. The btm employs *T* conformation and Hbtc^{2-} to generate a 1-D double-chain structure. The bte employs *T* conformation and H_2btc^{-} to give **2** as a 1-D chain. The flexible btp has the *GT* conformation and H_2btc^{-} also generates a 1-D chain in **3**. Solids **2** and **3** exhibit different patterns and space groups (*P*-1, **2**; *C*2/*c*, **3**) because of the varied conformations of bte and btp. Extended supramolecular architectures are constructed for these complexes via predictable secondary interactions such as hydrogen bonding and $\pi\cdots\pi$. Thus, tuning the organic spacer length is an effective strategy in crystal engineering to prepare inorganic –organic hybrid coordination polymers.

Supplementary material

CCDC-**1** 918157, CCDC-**2** 91858, and CCDC-**3** 91859 contain the Supplementary crystallographic data for this study. These data can be obtained free of charge via http://www.ccdc.cam.ac.uk/conts/retrieving.html (or from the Cambridge Crystallographic Centre, 12 Union Road, Cambridge CB21EZ, UK; Fax: +44 1223 336033; or E-mail: deposit@ccdc.cam.ac.uk).

Acknowledgment

This work was financially supported by the Natural Science Foundation of Tianjin (No. 12JCZDJC27600), P.R. China.

References

[1] T. Savaki, T. Dewa, Y. Aoyama. *J. Am. Chem. Soc.*, **120**, 8539 (1998).
[2] O. Ikkala, G. Brinke. *Science*, **295**, 2407 (2002).
[3] N. Ishikava, M. Sugita, T. Ishikawa, S.Y. Koshihara, Y. Kaizu. *J. Am. Chem. Soc.*, **125**, 8694 (2003).
[4] J.P. Zhang, Y.Y. Lin, W.X. Zhang, X.M. Chen. *J. Am. Chem. Soc.*, **127**, 14162 (2005).
[5] S. Kitagawa, S.I. Noro, T. Nakamura. *Chem. Commun.*, **11**, 701 (2006).
[6] J. Zhang, X.H. Bu. *Angew. Chem. Int. Ed.*, **46**, 6115 (2007).
[7] W. Morris, C.J. Doonan, H. Furukawa, R. Banerjee, O.M. Yaghi. *J. Am. Chem. Soc.*, **130**, 12626 (2008).
[8] N.W. Ockwig, O. Delgado-Friedrichs, M. O'Keeffe, O.M. Yaghi. *Acc. Chem. Res.*, **38**, 176 (2005).
[9] V.A. Friese, D.G. Kurth. *Coord. Chem. Rev.*, **252**, 199 (2008).
[10] K. Biradha, M. Sarkar, L. Rajput. *Chem. Commun.*, **11**, 4169 (2006).
[11] B.H. Ye, M.L. Tong, X.M. Chen. *Coord. Chem. Rev.*, **249**, 545 (2005).
[12] Y.Q. Huang, B. Ding, H.B. Song, B. Zhao, P. Ran, P. Cheng, H.G. Wang, D.Z. Liao, S.P. Yan. *Chem. Commun.*, **11**, 4906 (2006).
[13] X. Zhu, H. Ge, Y. Zhang, B. Li, Y. Zhang. *Polyhedron*, **25**, 1875 (2006).
[14] B. Ding, Y.Q. Huang, Y.Y. Liu, W. Shi, P. Cheng. *Inorg. Chem. Commun.*, **10**, 7 (2007).
[15] H.A. Habib, A. Hoffmann, H.A. Höppe, C. Janiak. *Dalton Trans*., 1742 (2009).
[16] D.F. Sun, R. Cao, Y.Q. Sun, W.H. Bi, X.J. Li, Y.Q. Wang, Q. Shi, X. Li. *Inorg. Chem.*, **42**, 7512 (2003).
[17] B. Li, X. Zhu, J. Zhou, Y. Peng, Y. Zhang. *Polyhedron*, **23**, 3133 (2004).
[18] X.Y. Wang, B.L. Li, X. Zhu, S. Gao. *Eur. J. Inorg. Chem.*, **2005**, 3277 (2005).
[19] C.D. Wu, W.B. Lin. *Angew. Chem. Int. Ed.*, **44**, 1958 (2005).
[20] L. Yi, X. Yang, T.B. Lu, P. Cheng. *Cryst. Growth Des.*, **5**, 1215 (2005).
[21] X. Zhu, H. Ge, Y. Zhang, B. Li. *Polyhedron*, **25**, 1875 (2006).
[22] L. Tian, Z.J. Zhang, A. Yu, W. Shi, Z. Chen, P. Cheng. *Cryst. Growth Des.*, **10**, 3847 (2010).
[23] L. Tian, N. Yang, G.Y. Zhao. *Inorg. Chem. Commun.*, **14**, 1497 (2010).
[24] L. Tian, L. Yan, S.Y. Liu. *J. Coord. Chem.*, **64**, 2945 (2011).
[25] L. Tian, Z. Niu, N. Yang, J.Y. Zou. *Inorg. Chim. Acta*, **370**, 230 (2011).
[26] J. Torres, J.L. Lavandera, P. Cabildo, R.M. Claramunt, J. Elguero. *J. Heterocycl. Chem.*, **25**, 771 (1988).
[27] S. Thakurta, P. Roy, G. Rosair, C.J.G. Garcia, E. Garribba, S. Mitra. *Polyhedron*, **28**, 695 (2009).